PHYSICAL REVIEW B **82**, 115203 (2010)

Piezospectroscopy of nitrogen-oxygen shallow donor complexes in silicon

H. Ch. Alt and H. E. Wagner
Department of Engineering Physics, University of Applied Sciences, Lothstrasse 34, 80335 Muenchen, Germany
(Received 29 June 2010; published 2 September 2010)

Electronic transitions of N-O related shallow donors in silicon doped with nitrogen and oxygen have been studied under uniaxial stress by Fourier transform spectroscopy in the far infrared. In first approximation, the stress dependence of the hydrogeniclike transitions is described by ground and excited state wave functions belonging to the T_2 representation of the tetrahedral group. Small splittings of the lines originate from the lifting of orientational degeneracy of low-symmetry centers. Nonlinear stress responses of some of the transitions are attributed to interactions with higher-lying 1*s* states. Full analysis of the two most prominent shallow donors N-O-3 and N-O-5 in terms of selection rules and line intensities under polarized light prove that the electronic states are perturbed by a defect potential of apparent C_{2v} symmetry, related to centers with an alignment along the ⟨110⟩ and a twofold symmetry axis along the ⟨001⟩ lattice direction. The donor wave function itself can be constructed from Bloch states belonging to a single pair of conduction band minima. It is concluded that present theoretical models for the microstructure of these complexes must be reconsidered, taking into account that any deviations from C_{2v} symmetry must be small and have no measurable effect on the stress pattern.

DOI: 10.1103/PhysRevB.82.115203 PACS number(s): 61.72.−y, 78.40.−q

I. INTRODUCTION

Nitrogen-related defects in silicon crystals grown by Czochralski (Cz) or floating zone (FZ) methods are of particular interest because of their impact on intrinsic point defects and defect agglomerates.[1,2] Nitrogen-oxygen complexes occur in nitrogen-doped Cz silicon crystals. Two different types of defects are known so far. One species is closely related to the dominant nitrogen defect in silicon, the nitrogen di-interstitial pair (NN).[3–6] They are generated by the interaction of the NN defect with one or two interstitial oxygen atoms (O_i) and are called NNO_n ($n=1,2$).[7–10] Experimentally, they show up by local vibrational mode absorption bands near the two fundamental vibrational modes of the NN defect at 967 and 770 cm^{-1} (at low temperatures). The NNO_n complexes are electrically inactive.

The other type of N-O complexes are centers with a core of one nitrogen atom and one or more oxygen atoms (NO_n, $n \geq 1$). They act as shallow donors (SD) and exhibit at low temperature (~10 K) sharp electronic transitions in the far infrared (FIR) between 180 and about 300 cm^{-1}. These so-called shallow (thermal) donors have been detected first in Cz silicon,[11–14] sometimes intentionally nitrogen doped and sometimes not, and later in Cz silicon annealed at high temperatures under nitrogen atmosphere.[15] In fact, these centers form a family of slightly different defects with at least eight members.[12,13,16] In cases, when they are present in the material, they are the shallowest donors, with binding energies between 34 and 38 meV.

The origin of these centers has been ambiguous for a long time, even the involvement of nitrogen as a part of their microscopic structure has been questioned.[14,16] The situation has become clearer when Voronkov *et al.*[17] showed that in well-defined samples, taken from Cz silicon crystals intentionally doped with nitrogen by adding silicon nitride to the melt and annealed between 600 and 650 °C, the SD concentration has a square-root relation to the total chemical nitrogen concentration, as determined by highly sensitive secondary ion mass spectroscopy. Also in this same paper, a thermodynamic model for the generation of these centers was developed, based on mass action laws and taking into account the crucial experimental observation. Within this model, the initial step is the binding of atomic nitrogen, the secondary fraction of nitrogen dissolved in the lattice, with interstitial oxygen. The different species of the SD family were explained qualitatively as being due to different numbers of interstitial oxygen atoms involved.

Also of importance is the work of Hara *et al.*[18,19] who investigated N-O SD complexes by electron spin resonance (ESR). Although the different members of the family cannot be resolved by this method, the conclusion could be drawn that the overall symmetry of SD centers is C_{2v}. Furthermore, they found that the ESR spectrum of N-O SD complexes is identical to the previously reported NL10 spectrum.[20]

First attempts to throw light on the structure of N-O SD complexes from a theoretical point of view go back to Jones *et al.*[21] They considered a planar O-N-O model with C_{2v} symmetry, consisting of a pair of over-coordinated O atoms binding with a substitutional N core atom. Later Ewels *et al.*[22] evaluated several structurally different NO_n defects and proposed that NO_2, also planar and with C_{2v} symmetry but now with an interstitial N core atom, is the most stable center and builds up the SD family. Further members of the defect family should be generated by binding with symmetrically added interstitial oxygen pairs. The idea of a four member N-O ring—very similar to the NN-pair structure—as the core structure of an N-O SD defect came from Gali *et al.*,[23] together with the suggestion that further interstitial oxygen atoms can be attracted to create the N-O SD family. Because the oxygen atom in the ring has one unpaired electron, the shallow donor property of this structural model is obvious. However, in conflict with ESR results and unlike the other models, symmetry is only monoclinic.

Systematic investigations of the thermal equilibrium concentrations of N-O SD centers in Cz crystals with varying

nitrogen and oxygen concentrations by measuring the strength of the FIR transitions showed that the major members of the N-O SD family all contain one nitrogen atom but different numbers of oxygen atoms.[24] More important, species with *both* even *and* odd numbers of oxygen atoms must exist. The chemical composition of all SD centers with respect to the number of oxygen atoms incorporated could finally be derived by an extension of these studies on a crystal with a large axial gradient of the O_i concentration, grown by a special oxygen-doping technology.[25] The result was that the center with the highest donor binding energy is chemically NO, the center with the highest concentration after annealing between 600 and 650 °C is NO_2.[26,27] These assignments seem to support the N-O ring model of Gali *et al.*[23] Recent improved calculations confirmed that this structure is energetically favorable.[28] Furthermore, the binding with one or more additional oxygen atoms leads to a series of successively shallower donor levels, in general accordance with our experimental observations.

Starting from this situation, additional experimental information about the microscopic structure of N-O SD centers is urgently needed. Uniaxial stress leads to the removal of orientational degeneracy of low-symmetry centers. From the splitting patterns of the FIR transitions in ⟨100⟩, ⟨111⟩, and ⟨110⟩ crystallographic directions, it should be possible to derive the symmetry of the donor wave function and, therefore, to obtain valuable information about the microstructure. In contrast to ESR measurements, IR absorption spectroscopy is able to determine the symmetry of each SD center separately. In this paper we present the results of the piezospectroscopic investigations on the species N-O-3 and N-O-5,[29] the centers with the strongest FIR transitions.

II. EXPERIMENTAL DETAILS

Samples for piezospectroscopic experiments were prepared from a FZ crystal grown by a special technique allowing selective doping with both nitrogen and oxygen.[25] Nitrogen and oxygen concentrations were 4×10^{14} cm^{-3} and 6×10^{17} cm^{-3}, respectively. Additionally, a background contamination with phosphorous and boron at a level of $<10^{14}$ cm^{-3} was present, leading to a slight *n*-type conductivity already before heat treatment. Thermal annealing was carried out at 600 °C for 7 h under nitrogen atmosphere to generate N-O SD defects at high concentrations.[17] A rapid thermal annealing device (Xerion XREACT) was used for high-temperature processing because it allows samples to be cooled down within a few minutes to uncritical temperature regions with regard to the formation of parasitic defects, such as oxygen-related thermal donors.[30] The total concentration of N-O SD centers was estimated to be around 10^{14} cm^{-3}.

Orientation of samples in ⟨100⟩, ⟨111⟩, and ⟨110⟩ directions was performed by the light-scattering method[31] or, alternatively, by x-ray diffraction. The accuracy of orientation was about 0.5° for the optical method and slightly better for x-ray diffraction, as estimated from the well-known stress-induced splitting of the phosphorous $1s\rightarrow2p_0$ and $1s\rightarrow2p_\pm$ transitions.[32,33] The size of the samples was between $3\times3\times12$ and $5\times6\times25$ mm^3. Uniaxial stress up to 0.25 GPa was applied by a home-made push-rod apparatus, conceptually similar to the construction of Tekippe *et al.*[34] The force was provided by a pneumatic piston. The absolute value of stress was set by N_2 gas pressure on the low-pressure side and the known pressure-intensifier ratio. Again from comparison with the stress-induced splitting of the phosphorous transitions, the accuracy of the stress setting was determined to be better than 5%.

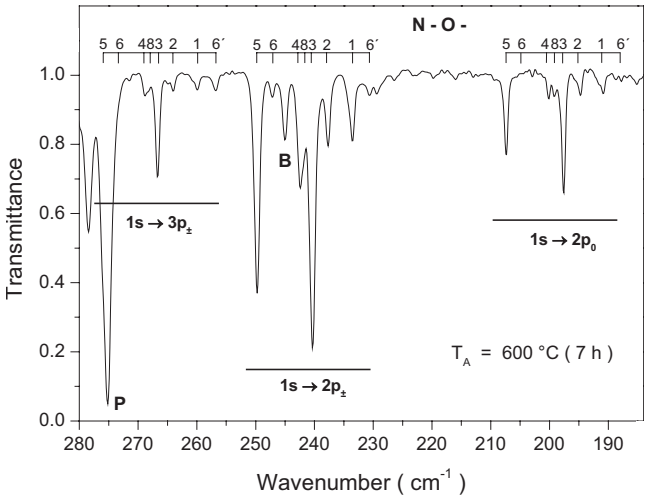

FIG. 1. Transmittance spectrum at 10 K in the spectral range of the N-O shallow donor $1s\rightarrow2p_0$ up to $1s\rightarrow3p_\pm$ transitions. Notation of the different donor species is according to Refs. 12 and 27.

Fourier transform infrared (FTIR) measurements were carried out with vacuum instrument (Bruker IFS 113v) equipped with a globar IR light source and a Si bolometer detector. A polyethylene polarizer and a Mylar beam splitter were used to obtain polarized spectra in the FIR region from 180–300 cm^{-1}. The sample temperature was 10 ± 1 K, the spectral resolution 0.3 or 0.5 cm^{-1}.

III. RESULTS AND DISCUSSION

A. General remarks

A typical FIR transmission spectrum at a sample temperature of 10 K in the range of the N-O shallow donor transitions is shown in Fig. 1. We observe eight different species of shallow donors: N-O-1, −2, −3, −4, −5, −6, 6′, and 8.[12,27] $1s\rightarrow2p_0$ transitions are in the range from 190 to 210 cm^{-1}, $1s\rightarrow2p_\pm$ transitions from 230 to 250 cm^{-1}, and $1s\rightarrow3p_\pm$ transitions from 255 to 275 cm^{-1}. Transitions to higher excited states are weaker, overlapping and not clearly resolved. They will not be considered further. The strongest lines in each group are those caused by N-O-3 and N-O-5. N-O-5 is considered as the primary defect of the N-O SD family and has the chemical composition NO.[26,27] N-O-3 has the composition NO_2 and is generated from N-O-5 by binding of an additional interstitial oxygen atom.[28]

We monitor the stress-induced shifts and splittings of the $1s\rightarrow2p_0$ transitions of N-O-3 and N-O-5 at 197.9 cm^{-1} and 207.4 cm^{-1}, respectively, and the $1s\rightarrow2p_\pm$ transitions of the same species at 240.4 cm^{-1} and 249.8 cm^{-1}, respectively.

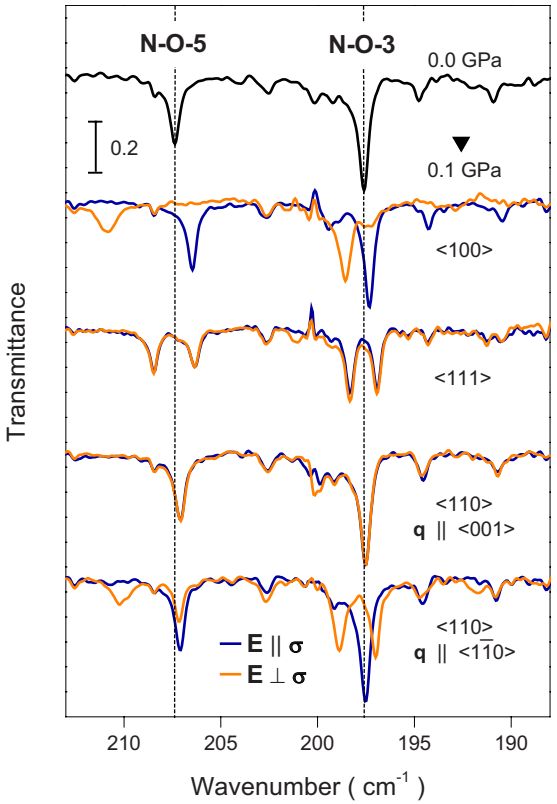

FIG. 2. (Color online) $1s \rightarrow 2p_0$ transitions of N-O-3 and N-O-5 for a stress of 0.1 GPa in the ⟨100⟩, ⟨111⟩, and ⟨110⟩ directions.

B. $1s \rightarrow 2p_0$ transitions

The behavior of the $1s \rightarrow 2p_0$ transitions under uniaxial stress in the ⟨100⟩, ⟨111⟩, and ⟨110⟩ directions is shown in Fig. 2. The first observation is that the stress-induced shifts and splittings are very small. They are of the order of 1 cm^{-1} per 0.1 GPa, far lower than the relevant shifts of the conduction band minima of silicon. Using the value of 8.77 eV for the shear-deformation potential constant Ξ_u, the splitting between the conduction band minima in the directions parallel and perpendicular to a stress of 0.1 GPa in ⟨100⟩ direction is about 69 cm^{-1}.[32,34] Accordingly, the splitting between the two components of the $1s \rightarrow 2p_0$ transition of arsenic, as an example for a typical shallow donor in silicon, for this stress is about 70 cm^{-1}.[33]

Therefore, N-O centers do *not* show this typical effective-masslike stress response, in spite of the fact that their binding energy is closest to the effective-mass value. The small splittings shown in Fig. 2 are due to the effect of a weak low-symmetry defect potential on the extended donor wave function and, therefore, on the transition energy. These splittings reflect the lifting of orientational degeneracy by uniaxial stress and have been treated theoretically by Kaplyanskii.[35] Indeed, the splittings are not only quantitatively but also qualitatively different from those of the conduction band minima: For a stress in ⟨111⟩ direction no splitting of the six ⟨100⟩ conduction band minima occurs because they all have the same direction cosine with ⟨111⟩. Therefore, no splitting of $1s \rightarrow 2p_0$ transitions should occur. However, in our case there is a splitting into two lines (Fig. 2).

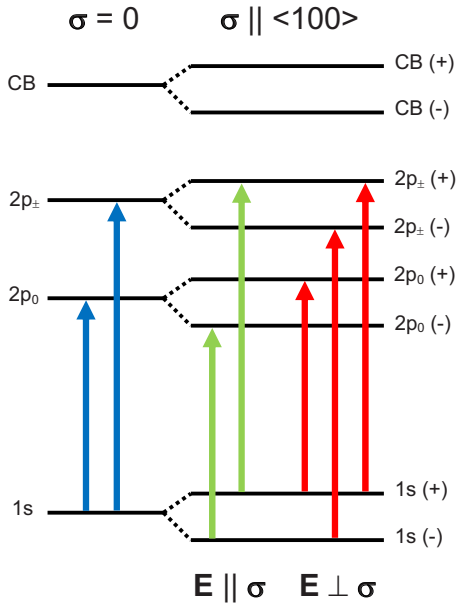

FIG. 3. (Color online) Splitting of the donor levels for a $1s(T_2)$ ground state under compressive stress in ⟨100⟩ direction. Allowed optical transitions for both polarization directions are shown as vertical arrows.

In first approximation, the observed behavior can be explained if it is assumed that the ground state of N-O shallow donors belongs to the T_2 representation of the tetrahedral group $[1s(T_2)]$, unlike the usual substitutional donors (As, P, Sb) which all have a $1s(A_1)$ ground state. In the case of a T_2 ground state the transition energy remains unchanged, because the ground state and the $2p_0$ excited state show exactly the same stress-induced splitting. The selection rules for the dipole transitions have been worked out by Aggarwal *et al.*[36] and are shown in Fig. 3. One comparable case of a shallow donor with a T_2 ground state has been reported in literature: The oxygen-related thermal double donors in Cz silicon. An extensive investigation of these defect states by FTIR piezospectroscopy has been carried out by Stavola *et al.*[37,38] It is claimed that the ground state wave function is constructed from a single pair of Bloch functions, belonging to two conduction band minima situated opposite in **k** space. We will show in the following that the N-O SD family exhibits many similarities with the O-related thermal donors.

The shifts and splittings for the $1s \rightarrow 2p_0$ transitions as a function of applied stress are shown in Fig. 4. Some of the stress dependences are obviously nonlinear. As Kaplyanskii's theory is a linear perturbation theory, this behavior needs particular discussion. We will do this separately in Sec. III D. Related to this phenomenon, those lines showing a strong nonlinearity become broader with increasing stress and can only be traced in a limited stress range. This applies particularly to the upper branch in ⟨100⟩ stress direction which is hardly evaluable beyond 0.1 GPa.

For both N-O-3 and N-O-5 we observe splitting of the $1s \rightarrow 2p_0$ transition into two branches for stress parallel to ⟨100⟩, two branches for stress parallel to ⟨111⟩, and three branches for stress parallel to ⟨110⟩. The latter direction exhibits a somewhat complicated stress pattern. One branch

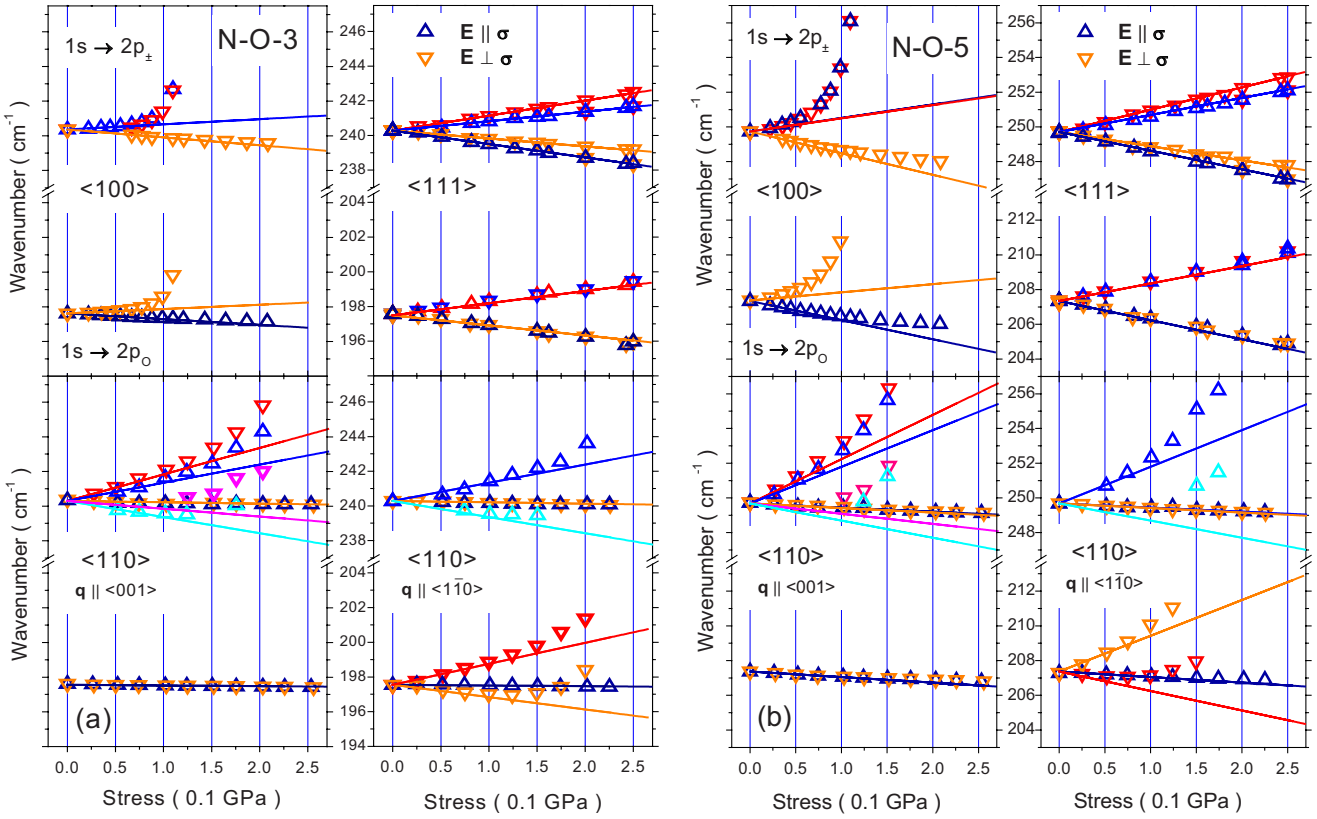

FIG. 4. (Color online) Transition frequencies of the different $1s \rightarrow 2p_0$ and $1s \rightarrow 2p_{\pm}$ branches for (a) N-O-3 and (b) N-O-5 as a function of stress.

with a linear and weakly negative stress dependence is observed for both polarizations parallel ($\mathbf{E} \| \boldsymbol{\sigma}$) and perpendicular to the stress direction ($\mathbf{E} \perp \boldsymbol{\sigma}$) in the case of light propagation in $\langle 001 \rangle$ direction. Three branches are resolved for light propagation in $\langle 1\bar{1}0 \rangle$ direction, including the same (central) branch for $\mathbf{E} \| \boldsymbol{\sigma}$ and, additionally, two branches above and below for $\mathbf{E} \perp \boldsymbol{\sigma}$. This can be seen clearly for N-O-3 and less obviously for N-O-5. The origin is the stress response of the low-frequency branch for $\mathbf{E} \perp \boldsymbol{\sigma}$. In the case of N-O-3 this branch starts for low stresses with the most negative stress coefficient, then becomes nonlinear with a convex curvature and crosses the central branch at about 0.17 GPa, and finally reappears on the high-wave-number side. In the case of N-O-5, the same branch nearly coincides with the central branch for low stresses and separates only above 0.1 GPa due to the nonlinear positive shift. However, polarization allows the tracking of the branch through the whole stress range.

From Kaplyanskii's tabulation[35] it is immediately clear that the number of branches in the different crystallographic directions is compatible with the lifting of the orientational degeneracy for centers with rhombic symmetry (rhombic I). The (linear) frequency shift Δ is calculated from the expression

$$\Delta = A_2\sigma_{xx} + A_2\sigma_{yy} + A_1\sigma_{zz} + 2A_3\sigma_{xy}. \quad (1)$$

The σ_{ij} are the components of the stress tensor and A_1, A_2, and A_3 the three independent parameters of the piezospectroscopic tensor. Due to the nonlinearities observed in $\langle 100 \rangle$ and $\langle 110 \rangle$ stress directions, we tried to fit the parameters only to the initial slope of the branches. This works very satisfactorily in the case of N-O-3 because the stress dependences have a linear part at low stresses. The result of the fit is $A_1 = -3.3$ cm^{-1}/GPa, $A_2 = 2.5$ cm^{-1}/GPa, and $A_3 = 9.6$ cm^{-1}/GPa. For N-O-5 the procedure is less reliable, as the upper branch in $\langle 100 \rangle$ and the two nonlinear branches in $\langle 110 \rangle$ stress direction have no clearly separable linear parts. Therefore, in this case the fit was carried out using only the remaining linear branches. The best result for N-O-5 is $A_1 = -11.0$ cm^{-1}/GPa, $A_2 = 4.7$ cm^{-1}/GPa, and $A_3 = 15.9$ cm^{-1}/GPa. The fits are displayed in Fig. 4 as straight lines. For N-O-3 the agreement of the fit with the experimental data is good, for N-O-5 satisfying.

From splittings of the $1s \rightarrow 2p_0$ transitions under stress we infer that N-O-3 and N-O-5 behave like centers of C_{2v} symmetry. Indeed, we will now demonstrate that the intensity ratios of the different stress-split branches under polarized light are fully consistent with the model of a C_{2v} defect oriented in a $\langle 110 \rangle$ direction and a ground state wave function consisting of a single pair of Bloch states. This model has been developed for the analysis of the stress splitting of the oxygen thermal double donor in silicon.[37,38] For example, if the center has the particular orientation along the crystallographic [110] direction, the ground-state wave function is constructed from the two Bloch states belonging to the two k_z-axis conduction band minima. Two such pairs can be constructed, one symmetric and one antisymmetric, both belong-

TABLE I. Splittings, shifts, and relative intensities for $1s \rightarrow 2p_0$ transitions of N-O-3 and N-O-5 under uniaxial stress in the ⟨100⟩, ⟨111⟩, and ⟨110⟩ directions. Notation is according to Kaplyanskii (Ref. 31).

			Intensity		
Direction of stress, σ	Frequency shift, Δ	Multiplicity	Calculation	N-O-3	N-O-5
				$I_{\parallel}:I_{\perp}$	
⟨100⟩	$A_2\sigma$	4	0:2	0:1.9	0:2.0
	$A_1\sigma$	2	2:0	1.9:0	2.0:0
⟨111⟩	$1/3(A_1+2A_2+2A_3)\sigma$	3	1:1	1.1:1.1	1.4:1.4
	$1/3(A_1+2A_2-2A_3)\sigma$	3	1:1	1.0:1.0	1.2:1.1
				$I_{110}:I_{001}:I_{1\bar{1}0}$	
⟨110⟩	$(A_2+A_3)\sigma$	1	0:1:0	0:1.2:0	0:0.9:0
	$\frac{1}{2}(A_1+A_2)\sigma$	4	2:0:2	1.9:0:1.7	1.7:0:1.5
	$(A_2-A_3)\sigma$	1	0:1:0	0:1.1:0	0:0.7:0

ing to the A_1 representation in C_{2v} symmetry. Our results do not distinguish between them. Because optical selection rules forbid intervalley transitions, only transitions to excited states of the same pair are allowed. In this case, the dipole moment for the $1s \rightarrow 2p_0$ transition is uniquely determined and oriented parallel to [001] (along the C_2 axis of the center). Using this scheme for all possible defect orientations in ⟨110⟩ directions, the intensity ratios of Table I can be calculated. It should be noted that the same intensity ratios are obtained for the so-called "σ oscillator" in Kaplyanskii's notation. The agreement between the line intensities required from the model and those observed from measurements under polarized light is excellent.

C. $1s \rightarrow 2p_{\pm}$ transitions

The general behavior of the $1s \rightarrow 2p_{\pm}$ transitions of N-O-3 and N-O-5 under stress as to the size and kinds of shifts and splittings is similar to the $1s \rightarrow 2p_0$ case. Therefore, the conclusions drawn there remain valid. However, in detail the interpretation of the $1s \rightarrow 2p_{\pm}$ case is more difficult. We observe a splitting into two branches for stress parallel to ⟨100⟩, four branches for stress parallel to ⟨111⟩, and five branches for stress parallel to ⟨110⟩ (Figs. 4 and 5). Compared to the $1s \rightarrow 2p_0$ transitions, the same splitting into two branches occurs for stress in ⟨100⟩ direction, with a strongly nonlinear upper branch. In ⟨111⟩ direction we get a doublet with different polarization behavior instead of each of the two branches of the $1s \rightarrow 2p_0$ transition.

The most complicated stress-splitting pattern is observed in ⟨110⟩ direction. For the light propagation vector **q** parallel to the ⟨001⟩ direction, two branches of different polarization are detected with a strongly positive but nonlinear frequency shift (Fig. 4). The "central" branch has a slightly negative frequency shift and is observed in both polarization directions. Two further branches exist, again with different polarization behavior, with a more negative frequency shift. Some illustrative spectra of this detail are shown in Fig. 6. These latter two lines are not detectable at low stresses <0.05 GPa because of the overlap with the central line. In the range between 0.05 and 0.12 GPa the line observable for $\mathbf{E} \parallel \boldsymbol{\sigma}$ is detected in the case of N-O-3 as a small shoulder on the low-frequency side of the main band. The other line (observable for $\mathbf{E} \perp \boldsymbol{\sigma}$) is detected by peak fitting analysis in the case of N-O-3. For N-O-5 it becomes separated from the main band due to the strongly nonlinear positive frequency shift in the limited stress range between 0.1 and 0.2 GPa. The related drop of intensity of the main band is clearly visible in both cases.

The $1s \rightarrow 2p_{\pm}$ transitions differ from the $1s \rightarrow 2p_0$ transitions only by the final state. Therefore, one could speculate

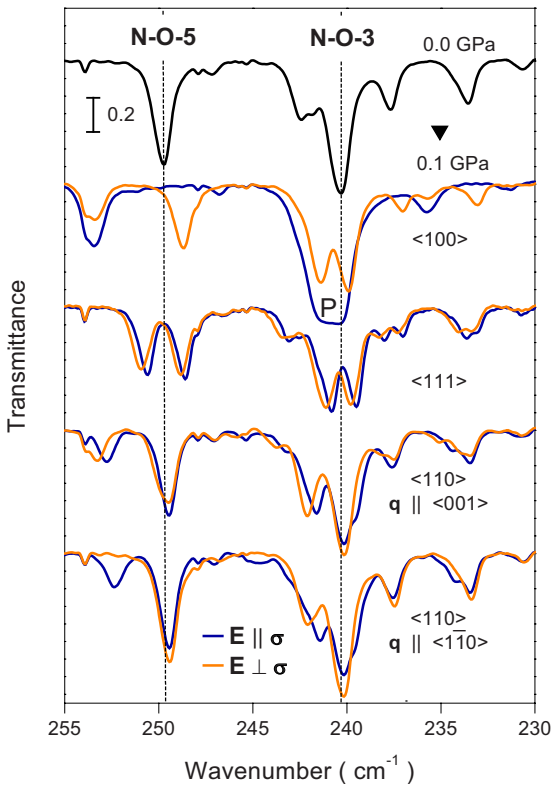

FIG. 5. (Color online) $1s \rightarrow 2p_{\pm}$ transitions of N-O-3 and N-O-5 for a stress of 0.1 GPa in the ⟨100⟩, ⟨111⟩, and ⟨110⟩ directions. Note that the line at about 242 cm^{-1} for $\sigma \parallel \langle 110 \rangle$ ($\mathbf{q} \parallel \langle 1\bar{1}0 \rangle$) and $\mathbf{E} \perp \boldsymbol{\sigma}$ is not related to N-O-3, but to N-O-4.

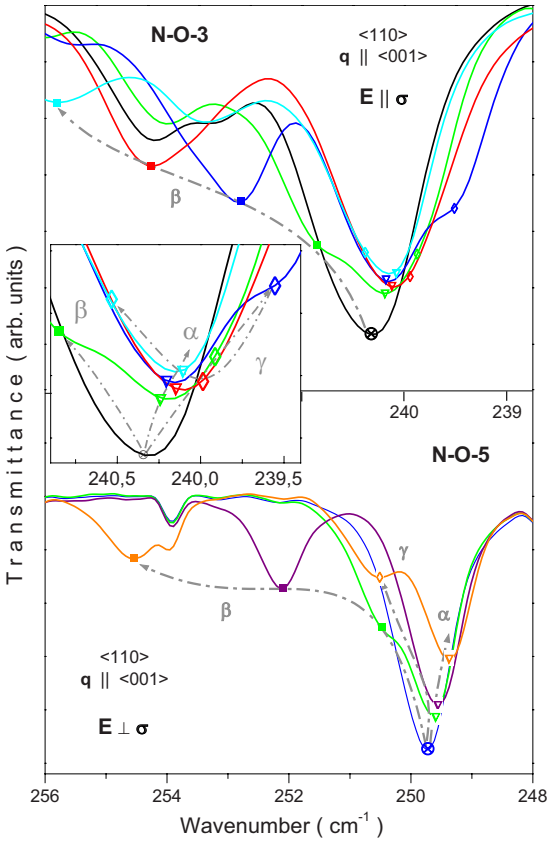

FIG. 6. (Color online) Details of the splitting of the $1s \rightarrow 2p_{\pm}$ transition under stress in $\langle 110 \rangle$ direction ($\mathbf{q} \| \langle 001 \rangle$). The upper panel with related inset shows the behavior of the transitions observable for polarization $\mathbf{E} \| \boldsymbol{\sigma}$, exemplified by N-O-3: central line α [stress dependence $\frac{1}{2}(A_1+A_2)\sigma$], high-frequency line β [$(A_2+A_3)\sigma$], and low-frequency line γ [$(A_2-A_3)\sigma$]. This latter line is visible only as a low-frequency shoulder of the main line for medium stress. The arrows visualize the shift of the lines as a function of (increasing) stress. The lower panel shows the same for polarization $\mathbf{E} \perp \boldsymbol{\sigma}$, in this case demonstrated by the transitions of N-O-5. Sequence of applied stresses is 0, 0.05, 0.1, 0.15, and 0.175 GPa for the upper and 0, 0.025, 0.075, and 0.125 GPa for the lower panel, respectively.

that the $2p_{\pm}$ wave functions "feel" a different defect symmetry than the $2p_0$ wave functions. Having a look into Kaplyanskii's tabulation,[35] it is evident that the clearly resolved four branches in $\langle 111 \rangle$ stress direction require a center with triclinic symmetry. In this case, the $\langle 110 \rangle$ direction would split into six branches. However, trying to fit the observed stress-splitting by a piezospectroscopic tensor with six independent components, leads to unsatisfying results. Moreover, the distinct polarization properties of the branches in $\langle 111 \rangle$ and $\langle 110 \rangle$ stress direction are difficult to explain for centers with triclinic symmetry. We therefore come to the conclusion that stress leads to a splitting of the $2p_{\pm}$ excited state itself. These states are orbitally degenerate for a center with T_d symmetry. However, there is no reason that this degeneracy should endure for centers with lower site symmetry. Indeed, also Stavola *et al.*[37,38] observed for the singly ionized charge state of the oxygen thermal double donors a splitting of the $np_{\pm}$ excited states, even at zero stress.

TABLE II. Compilation of the piezospectroscopic parameters for N-O-3 and N-O-5 obtained in this work.

Complex	Transition	A_1 (cm^{-1}/GPa)	A_2 (cm^{-1}/GPa)	A_3 (cm^{-1}/GPa)
N-O-3	$1s \rightarrow 2p_0$	−3.3	+2.5	+9.6
	$1s \rightarrow 2p_-$	−4.6	+3.0	+12.3
	$1s \rightarrow 2p_+$	−4.6	+3.0	+7.5
N-O-5	$1s \rightarrow 2p_0$	−11.0	+4.7	+15.9
	$1s \rightarrow 2p_-$	−12.5	+7.8	+17.7
	$1s \rightarrow 2p_+$	−12.6	+7.6	+13.5

The $1s \rightarrow 2p_-$ and $1s \rightarrow 2p_+$ transitions of N-O-3 and N-O-5 under uniaxial stress are therefore analyzed separately, on the basis of an assumed C_{2v} defect symmetry. The polarization behavior allows the unique assignment of each branch to the $2p_-$ or $2p_+$ final state, respectively, as will be shown below. Equation (1) is used for fitting. However, because of the strong nonlinearity and the uncertainty of the exact line positions at low stress in $\langle 110 \rangle$ direction, only the $\langle 100 \rangle$ and $\langle 111 \rangle$ directions were used to fit the piezospectroscopic parameters A_1, A_2, and A_3. Using this procedure, we get in the case of N-O-3 the values $A_1 = -4.6$ cm^{-1}/GPa, $A_2 = 3.0$ cm^{-1}/GPa, and $A_3 = 12.3$ cm^{-1}/GPa for the $1s \rightarrow 2p_-$ transition, and $A_1 = -4.6$ cm^{-1}/GPa, $A_2 = 3.0$ cm^{-1}/GPa, and $A_3 = 7.5$ cm^{-1}/GPa for the $1s \rightarrow 2p_+$ transition, respectively. For N-O-5 the fitted piezospectroscopic parameters are $A_1 = -12.5$ cm^{-1}/GPa, $A_2 = 7.8$ cm^{-1}/GPa, and $A_3 = 17.7$ cm^{-1}/GPa for the $1s \rightarrow 2p_-$ transition, and $A_1 = -12.6$ cm^{-1}/GPa, $A_2 = 7.6$ cm^{-1}/GPa, and $A_3 = 13.5$ cm^{-1}/GPa for the $1s \rightarrow 2p_+$ transition, respectively. A compilation of all determined piezospectroscopic parameters is given in Table II.

Both fits are compatible with the existing experimental data in all three stress directions (see fit lines in Fig. 4). Altogether, the fit is better for N-O-3 than for N-O-5. The reason is the strongly nonlinear behavior of the upper branch in $\langle 100 \rangle$ stress direction for N-O-5 making it impossible to determine reliably a (linear) initial slope. Due to the fact that the $1s \rightarrow 2p_-$ and $1s \rightarrow 2p_+$ transitions remain degenerate in $\langle 100 \rangle$ stress direction, the parameters A_1 and A_2 are the same for both transitions within experimental accuracy. For the $\langle 110 \rangle$ direction, the fits predict a branch with a moderately decreasing frequency for increasing stress. This branch has a stress dependence $\Delta = \frac{1}{2}(A_1+A_2)\sigma$ and is identical with the observed central branch showing a linear shift with stress. For N-O-3, the measured shift is -1.1 cm^{-1}/GPa. The fits predict -0.8 cm^{-1}/GPa for both the $1s \rightarrow 2p_-$ transition and the $1s \rightarrow 2p_+$ transition. In the case of N-O-5 the measured value is -2.6 cm^{-1}/GPa whereas the fit predicts -2.5 cm^{-1}/GPa for the $1s \rightarrow 2p_-$ transition and -2.3 cm^{-1}/GPa for the $1s \rightarrow 2p_+$ transition, respectively. Therefore the coincidence of this central branch for the $1s \rightarrow 2p_-$ and the $1s \rightarrow 2p_+$ transitions in $\langle 110 \rangle$ direction is obviously correctly reproduced. Furthermore, the fits predict in $\langle 110 \rangle$ direction a branch with a strongly positive frequency shift and a branch with a negative frequency shift. Here, a quantitative comparison with experiment is not possible be-

TABLE III. Splittings, shifts, and relative intensities for $1s \rightarrow 2p_-$ and $1s \rightarrow 2p_+$ transitions of N-O-3 and N-O-5 under uniaxial stress in the ⟨100⟩, ⟨111⟩, and ⟨110⟩ directions.

			Intensity[a]		
Direction of stress, σ	Frequency shift, Δ	Multiplicity	Calculation	N-O-3	N-O-5
				$I_{\parallel}:I_{\perp}$	
⟨100⟩	$A_2\sigma$	4	2:1	3.9:2.3	3.7: 2.3
			2:1		
	$A_1\sigma$	2	0:1	0:2.2	0:2.1
			0:1		
⟨111⟩	$1/3(A_1+2A_2+2A_3)\sigma$	3	0:3/2	0:1.3	0:1.5
			$2:\frac{1}{2}$	1.6:0.4	1.9:0.5
	$1/3(A_1+2A_2-2A_3)\sigma$	3	$2:\frac{1}{2}$	1.7:0.4	1.7:0.5
			0:3/2	0:1.4	0:1.4
				$I_{110}:I_{001}:I_{1\bar{1}0}$	
⟨110⟩	$(A_2+A_3)\sigma$	1	0:0:1	0:0:0.9	0:0:0.8
			1:0:0	1.4:0:0	1.0:0:0
	$\frac{1}{2}(A_1+A_2)\sigma$	4	1:2:1	1.9:4.9:2.3	1.9:4.9:1.9
			1:2:1		
	$(A_2-A_3)\sigma$	1	1:0:0	1.0:0:0	1.0:0:0
			0:0:1	0:0:0.6	0:0:0.9

[a]The first entry in each row describes the $1s \rightarrow 2p_-$ transition, the second the $1s \rightarrow 2p_+$ transition. In ⟨100⟩ stress direction, the two transitions remain energetically degenerate. Therefore the measured intensity must be compared with the sum of the calculated intensities for both transitions (assuming that the absolute value of the transition matrix element is the same). The same is true for the central branch in ⟨110⟩ direction $[\frac{1}{2}(A_1+A_2)\sigma]$.

cause of the strong nonlinearity and, additionally (for the lower branch), because of the overlap with the central branch.

As a further strong argument in favor of the proposed model, we present in Table III the analysis of the line intensities under polarized light. The calculation is analogous to the procedure outlined shortly in Sec. III B and presented in detail in Ref. 38. First, appropriate linear combinations of the $2p_\pm$ wave functions are constructed that transform in accordance with the B_1 and B_2 representations of the C_{2v} point group (For simplicity, we leave the notation of the new states unchanged.) For a center oriented along the [110] crystallographic direction, the optical transition dipole moments from the $1s$ initial to these final states lie along the [110] and $[1\bar{1}0]$ directions, respectively. Somewhat arbitrary, we assign the $1s \rightarrow 2p_+$ transition moment to the [110] direction, and the $1s \rightarrow 2p_-$ transition moment to the $[1\bar{1}0]$ direction. With these assignments, the expected relative intensities for the different transitions are calculated.

Within the experimental error, the agreement between the intensities calculated according to the model presented and those determined from our measurements is excellent. Particularly instructive is the ⟨111⟩ direction. Due to the different orientation of the dipole moment, the $1s \rightarrow 2p_-$ and $1s \rightarrow 2p_+$ transitions should have completely different intensities under polarized light. For the high-frequency $2p_-$ final state the intensity ratio for $\mathbf{E} \| \boldsymbol{\sigma}$ to $\mathbf{E} \perp \boldsymbol{\sigma}$ is 0: 3/2, for $2p_+$ correspondingly 2: 1/2. The related absorbance spectra are shown in Fig. 7 for a ⟨111⟩ stress of 0.25 GPa. It is clearly seen that for $\mathbf{E} \| \boldsymbol{\sigma}$ only two bands of equal intensity are observed, for $\mathbf{E} \perp \boldsymbol{\sigma}$ four lines with different intensities. The two weaker lines in this latter polarization direction coincide with the spectral position of the lines for $\mathbf{E} \| \boldsymbol{\sigma}$. The intensities evaluated from the data by peak-fitting procedure support the model on a quantitative basis (see Table III). Also

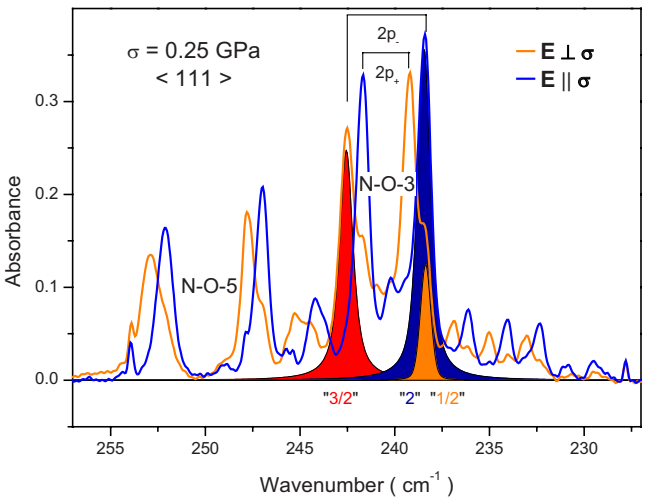

FIG. 7. (Color online) Detail of the line intensities of the $1s \rightarrow 2p_-$ and $1s \rightarrow 2p_+$ transitions for polarized light and stress in ⟨111⟩ direction. The colored areas correspond to the fitted line intensities given in Table III.

from this stress direction, it is deduced that the $2p_-$ state has the larger stress-induced shift in this direction (i.e., the larger A_3 coefficient).

It should be mentioned that also the $3p_\pm$ states split under $\langle 111 \rangle$ stress. The splitting is smaller than for the $2p_\pm$ states. Therefore, the spatially even more extended $3p_\pm$ wave functions are influenced by the low-symmetry defect core potential. The apparent defect symmetry is again C_{2v}.

D. Nonlinear stress dependences

A very unusual feature of the N-O SD complexes is the nonlinear stress response for some of the transitions (see Fig. 4). This is observed not only for N-O-3 and N-O-5, as discussed here, but also in a similar manner for all other members of the complex family. As the treatment of the stress response in the sense of Kaplyanskii is a weak perturbation approach and therefore necessarily a linear model, this behavior must be related to a different mechanism. The first obvious observation is that not all of the branches show this nonlinearity. In particular, for stress in $\langle 111 \rangle$ direction the stress dependences are perfectly linear. The lower branch in $\langle 100 \rangle$ direction and the central branch in $\langle 110 \rangle$ direction are also predominantly linear. A closer inspection of the affected transitions reveals that in $\langle 100 \rangle$ stress direction only transitions originating from the upper ground state level $1s(+)$ (Fig. 3) have a strongly nonlinear stress dependence. Also for the $\langle 110 \rangle$ direction it can be shown that the linear branch originates from the lower-lying $1s(-)$ ground state whereas all other branches comes from the upper one.[39]

The nonlinear effect is different for different donors. For N-O-3 the nonlinearity is unambiguously detectable (i.e., exceeds the experimental uncertainty) at about 0.08 GPa whereas for N-O-5 this is already the case for stresses greater than 0.05 GPa (Fig. 8). Therefore, the complex with the larger donor binding energy (N-O-5) shows the stronger nonlinearity. This tendency that the nonlinearity starts later with decreasing SD binding energy—although not shown here—can be experimentally pursued for further members of the N-O SD family, with weaker $1s \rightarrow 2p_\pm$ transitions on the low-frequency side of the strong N-O-3 transition at 240 cm^{-1}.

The second systematic behavior which can be extracted from the experiments is the fact that the nonlinearity is identical for all transitions of a specific donor. This is also shown in Fig. 8, where the transitions $1s \rightarrow 2p_0$, $1s \rightarrow 2p_\pm$, $1s \rightarrow 3p_\pm$, and $1s \rightarrow 4p_\pm$ of N-O-5 are compared. Therefore, the origin of the nonlinear behavior must be attributed to the ground state, not to the excited states of the donor electron.

Based on these experimental observations, the most probable explanation is that the ground state of the N-O SD electron interacts under compressive stress with energetically higher lying $1s$ states. Because of the six conduction band minima in silicon, there must also exist six $1s$ states. We observe at low temperatures only one of them, the energetically lowest-lying one. This interpretation is supported by the behavior under stress in $\langle 111 \rangle$ direction: For this stress direction all conduction band minima shift by the same amount, no splitting occurs. Also all states of the donor electron for a complex with a particular orientation in the lattice, ground state as well as excited states, keep their energetic distance, irrespective of the size of stress. Therefore no interaction between different $1s$ states can occur. This is reflected by the strictly linear stress response in $\langle 111 \rangle$ direction, up to the highest stresses applied (Fig. 4). On the other hand, for $\langle 100 \rangle$ stress direction, the upper $1s(+)$ ground state of the donor electron (Fig. 3) experiences a strongly positive shift with increasing stress. It must be expected that some of the higher-lying $1s$ states do not move in the same manner. Indeed, the shift of the T_2-like $1s$ states forming the ground state of the centers with the specific orientation giving rise to the upper branch for stress in $\langle 100 \rangle$ direction is the strongest positive shift in this direction.[36] A qualitatively similar argument holds for the $\langle 110 \rangle$ direction. Therefore, the two states involved—the ground state and the next higher-lying $1s$ state—approach each other and a typical quantum mechanical repulsion occurs. As a consequence, the ground state is pushed downwards and the experimentally observed transitions from the ground state to the excited states show an increase in energy.

It is not unreasonable to argue that the energetic difference between the ground state and the next higher lying $1s$ state varies systematically with the donor binding energy. This would explain the monotonic increase in the stress threshold for the onset of the nonlinear effect with decreasing donor binding energy. Experimentally, there is so far no

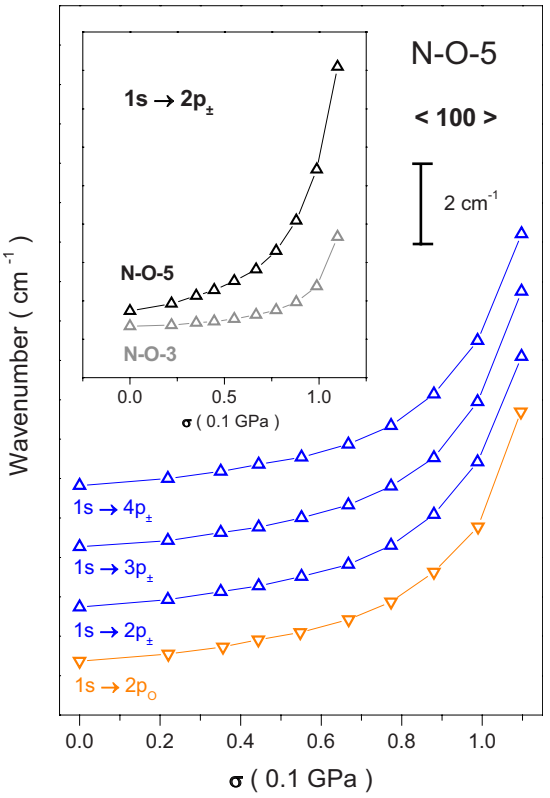

FIG. 8. (Color online) Characteristics of the nonlinear stress response for the different observable transitions of N-O-5 under stress in $\langle 100 \rangle$ direction. The transitions frequencies have been shifted for clarity. Inset shows comparison of the $1s \rightarrow 2p_\pm$ transitions for N-O-3 and N-O-5.

direct evidence of higher lying $1s$ states. This would require absorption measurements at higher temperatures, where these levels could be populated thermally. However, due to the small donor binding energy, the temperature range where this could happen, before complete ionization occurs, is very narrow and probably difficult to investigate.

E. Thermal ionization

An independent method to check the consistency of the proposed model of a T_2-like donor ground state that splits under uniaxial stress exactly like the excited states and the corresponding conduction band minima without considering the lifting of orientational degeneracy, is the investigation of the thermal ionization process. The idea has been proposed and experimentally confirmed by Stavola *et al.*[37,38] for the case of the oxygen thermal double donors. The splitting between the $1s(+)$ and the $1s(-)$ ground state for a compressive stress of 0.1 GPa in $\langle 100 \rangle$ direction is 69 cm^{-1} or 8.6 meV.[32,34] This is a considerable fraction of the donor binding energy of 36.2 and 37.4 meV for N-O-3 and N-O-5,[12] respectively. Therefore, when raising the sample temperature under compressive stress, electrons from the upper $1s(+)$ level should ionize earlier than those from the lower $1s(-)$ level. Alternatively, one can apply stress at a temperature where (at zero stress) already partial ionization occurs. In this case, the lower $1s(-)$ level will be filled up again at the cost of the upper $1s(+)$ level.

This is indeed observed, as can been seen in Fig. 9 for a sample temperatures of 22 K. At this temperature the equilibrium occupation of the N-O-3 ground state is about 2/3. The intensity of the $1s \rightarrow 2p_0$ transition with the higher frequency, starting from the $1s(+)$ ground state, obviously decays for increasing $\langle 100 \rangle$ stress whereas that of the low-frequency transition grows. More quantitatively, the ionization process is described by the ratio of occupied and ionized donors states $N_{D,0}/N_{D,+}$ as

$$N_{D,0}/N_{D,+} = \exp[-(E_D - E_F)/kT] \qquad (2)$$

with the donor binding energy and the Fermi energy E_D and E_F, respectively. As the position of the Fermi energy in our samples is not exactly known and probably changes during the thermal redistribution process under stress, it is more convenient for the evaluation to take expression (2) for both the upper and the lower branch, and calculate the ratio r as

$$r = \{N_{D,0}/N_{D,+}\}_u / \{N_{D,0}/N_{D,+}\}_l = \exp[-\Delta E_D/kT] \qquad (3)$$

where u and l stands for upper and lower branch, respectively, and ΔE_D is the energy splitting between the $1s(+)$ and the $1s(-)$ ground state under stress.

The values for $N_{D,0}$ were determined directly from the line intensity under stress, those for $N_{D,+}$ from the decrease in the intensity with respect to 10 K value, where complete occupation can be assumed. The result of such an analysis, presented as a logarithmic plot, is also shown in Fig. 9. From the slope of the ratio r versus stress σ a value of about 500 cm^{-1}/GPa is derived for $\Delta E_D/\sigma$. Within the experimental uncertainty of about 10% for the determination of the line intensities, this value is in reasonable agreement with the splitting of the conduction band under stress in $\langle 100 \rangle$ direction. Therefore, this experiment confirms that the experimentally observed transitions stem from different T_2-like ground states, stress-split by an energy much larger than observed directly in the stress panels (Fig. 4).

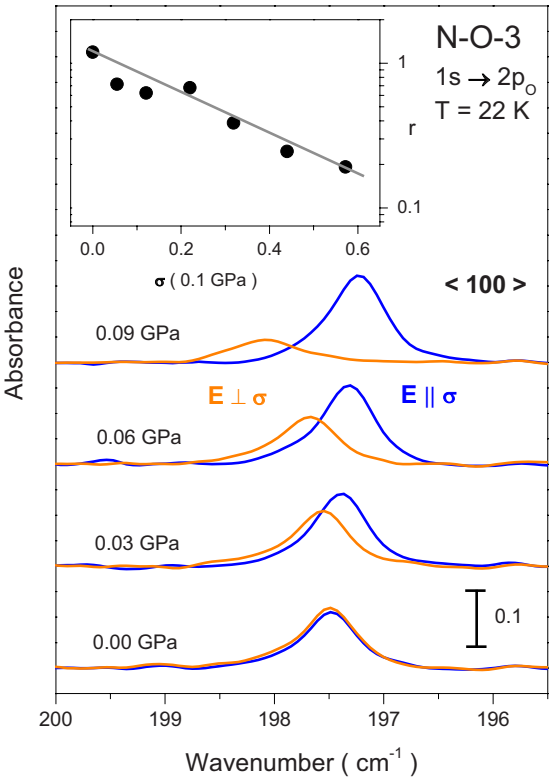

FIG. 9. (Color online) Intensities of the $1s \rightarrow 2p_0$ transitions of N-O-3 at an elevated sample temperature of 22 K as a function of stress in $\langle 100 \rangle$ direction. Inset shows logarithmic plot of the intensity ratio r (see text for further details) as a function of stress σ.

IV. CONCLUSIONS

Uniaxial stress investigations reveal that the N-O shallow donor electron has a very peculiar ground state wave function. It can be modeled by a single pair of Bloch states derived from two conduction band minima situated opposite in **k** space. Therefore, and because intervalley transitions are forbidden, ground state and excited states undergo the same conduction-band related shift caused by stress, cancelling out when transitions between these states are studied. However, the ground states associated with different pairs of conduction band minima can be detected indirectly by thermal ionization and redistribution experiments at elevated sample temperatures. Ground states belonging to energetically higher-lying conduction bands are depopulated under stress, those belonging to lower-lying bands filled up.

Small splittings of the $1s \rightarrow 2p_0$ and $1s \rightarrow 2p_\pm$ transitions are observed that are due to lifting of orientational degeneracy. The detailed analysis of these splittings for the N-O-3 and N-O-5 centers in terms of polarization dependent intensities is fully consistent with donor wave functions belonging to complexes of C_{2v} symmetry. Ground and excited states

respond sensitively and differently to the interaction with the anisotropic defect core and are described by different sets of piezospectroscopic parameters. This leads to splitting of the $2p_{\pm}$ states under stress.

Our results are in agreement with the earlier ESR studies of Hara *et al.*,[18] where C_{2v} symmetry was found for the nitrogen-oxygen shallow donor electron. However, as spin resonance cannot resolve the different species of the N-O family, this result must be considered as a kind of averaging over different members of the family. We demonstrate that the most prominent centers after an annealing process at 600 °C, N-O-3 and N-O-5, have individually a ground state wave function of C_{2v} symmetry.

It is felt that present theoretical models for the microstructure of these complexes are not compatible with our results. The model of Gali *et al.*[23] for the NO complex, with its core of an N-O ring in the {110} plane, is a distinctly monoclinic configuration (C_{1h} symmetry). This structure has been recalculated recently and affirmed, together with a closely related monoclinic structure for NO_2.[28] By contrast, the earlier model for NO_2 of Ewels *et al.*[22] with two interstitial oxygen atoms placed symmetrically on either side of the nitrogen atom has C_{2v} symmetry. However, this structure does not allow an NO complex which is the chemical composition of N-O-5 according to our own results.[26,27]

In principle, there are two possibilities: the donor wave function does indeed not "feel" the low-symmetry (monoclinic) part of the defect potential or the microstructure of N-O complexes (at least for NO) must be reconsidered. The first scenario appears unlikely, given the fact that obviously not only the ground-state energy but also the wave function (in terms of the stress response) are sensitively dependent on modifications of the N-O microstructure. Ground state and excited states, at least up to the $3p_{\pm}$ state, are influenced by the low-symmetry defect potential—differently in strength but always in consistence with a C_{2v} defect symmetry.

ACKNOWLEDGMENTS

The authors are indebted to W. v. Ammon for providing some of the samples. We would also like to thank B. Clerjaud for giving some hints about uniaxial stress spectroscopy experiments. Part of this work was funded by the Deutsche Forschungsgemeinschaft (DFG).

[1] W. von Ammon, R. Hölzl, J. Virbulis, E. Dornberger, R. Schmolke, and D. Gräf, J. Cryst. Growth **226**, 19 (2001).
[2] K. Nakai, Y. Inoue, H. Yokota, A. Ikari, J. Takahashi, K. Kitahara, Y. Ohta, and W. Ohashi, J. Appl. Phys. **89**, 4301 (2001).
[3] H. J. Stein, Appl. Phys. Lett. **47**, 1339 (1985).
[4] R. Jones, S. Öberg, F. Berg Rasmussen, and B. Bech Nielsen, Phys. Rev. Lett. **72**, 1882 (1994).
[5] F. B. Rasmussen and B. B. Nielsen, Phys. Rev. B **49**, 16353 (1994).
[6] F. B. Rasmussen and B. B. Nielsen, Mater. Sci. Eng., B **36**, 241 (1996).
[7] P. Wagner, R. Oeder, and W. Zulehner, Appl. Phys. A: Mater. Sci. Process. **46**, 73 (1988).
[8] M. W. Qi, S. S. Tan, B. Zhu, P. X. Cai, W. F. Gu, X. M. Xu, T. S. Shi, D. L. Que, and L. B. Li, J. Appl. Phys. **69**, 3775 (1991).
[9] R. Jones, C. Ewels, J. Goss, J. Miro, P. Deak, S. Öberg, and F. Berg Rasmussen, Semicond. Sci. Technol. **9**, 2145 (1994).
[10] F. B. Rasmussen, S. Öberg, R. Jones, C. Ewels, J. Goss, J. Miro, and P. Deák, Mater. Sci. Eng., B **36**, 91 (1996).
[11] H. Navarro, J. Griffin, J. Weber, and L. Genzel, Solid State Commun. **58**, 151 (1986).
[12] M. Suezawa, K. Sumino, H. Harada, and T. Abe, Jpn. J. Appl. Phys., Part 2 **25**, L859 (1986).
[13] M. Suezawa, K. Sumino, H. Harada, and T. Abe, Jpn. J. Appl. Phys. **27**, 62 (1988).
[14] J. A. Griffin, J. Hartung, J. Weber, H. Navarro, and L. Genzel, Appl. Phys. A: Mater. Sci. Process. **48**, 41 (1989).
[15] A. Hara, T. Fukuda, T. Miyabo, and I. Hirai, Appl. Phys. Lett. **54**, 626 (1989).
[16] R. C. Newman, J. H. Tucker, N. G. Semaltianos, E. C. Lightowlers, T. Gregorkiewicz, I. S. Zevenbergen, and C. A. J. Ammerlaan, Phys. Rev. B **54**, R6803 (1996).
[17] V. V. Voronkov, M. Porrini, P. Collareta, M. G. Pretto, R. Scala, R. Falster, G. I. Voronkova, A. V. Batunina, V. N. Golovina, L. V. Arapkina, A. S. Guliaeva, and M. G. Milvidski, J. Appl. Phys. **89**, 4289 (2001).
[18] A. Hara, T. Fukuda, T. Miyabo, and I. Hirai, Jpn. J. Appl. Phys. **28**, 142 (1989).
[19] A. Hara, I. Hirai, and A. Ohsawa, J. Appl. Phys. **67**, 2462 (1990).
[20] T. Gregorkiewicz, D. A. van Wezep, H. H. P. Th. Bekman, and C. A. J. Ammerlaan, Phys. Rev. B **35**, 3810 (1987).
[21] R. Jones, S. Öberg, and A. Umerski, Mater. Sci. Forum **65-66**, 287 (1991).
[22] C. P. Ewels, R. Jones, S. Öberg, J. Miro, and P. Deak, Phys. Rev. Lett. **77**, 865 (1996).
[23] A. Gali, J. Miro, P. Deak, C. P. Ewels, and R. Jones, J. Phys.: Condens. Matter **8**, 7711 (1996).
[24] H. Ch. Alt, Y. V. Gomeniuk, F. Bittersberger, A. Kempf, and D. Zemke, Appl. Phys. Lett. **87**, 151909 (2005).
[25] W. v. Ammon, A. Ehlert, and W. Hensel, in *Crystalline Defects and Contamination: Their Impact and Control in Device Manufacturing*, The Electrochemical Society Proceedings Series, edited by B. O. Kolbesen, C. Claeys, P. Stallhofer, and F. Tardif (Pennington, NJ, 1993), pp. 36–50.
[26] H. Ch. Alt, H. E. Wagner, W. v. Ammon, F. Bittersberger, A. Huber, and L. Koester, Physica B **401-402**, 130 (2007).
[27] H. E. Wagner, H. Ch. Alt, W. von Ammon, F. Bittersberger, A. Huber, and L. Koester, Appl. Phys. Lett. **91**, 152102 (2007).
[28] N. Fujita, R. Jones, S. Öberg, and P. R. Briddon, Appl. Phys. Lett. **91**, 051914 (2007).
[29] Notation of the N-O SD donor species is according to Ref. 12.
[30] H. Ch. Alt and H. E. Wagner, J. Appl. Phys. **106**, 103511 (2009).
[31] R. D. Hancock and S. Edelman, Rev. Sci. Instrum. **27**, 1082 (1956).
[32] C. Herring and E. Vogt, Phys. Rev. **101**, 944 (1956).

[33] C. Jagannath and A. K. Ramdas, Phys. Rev. B **23**, 4426 (1981).
[34] V. J. Tekippe, H. R. Chandrasekhar, P. Fisher, and A. K. Ramdas, Phys. Rev. B **6**, 2348 (1972).
[35] A. A. Kaplyanskii, Opt. Spectrosc. **16**, 329 (1964).
[36] R. L. Aggarwal, P. Fisher, V. Mourzine, and A. K. Ramdas, Phys. Rev. **138**, A882 (1965); R. L. Aggarwal and A. K. Ramdas, *ibid.* **140**, A1246 (1965).
[37] M. Stavola, K. M. Lee, J. C. Nabity, P. E. Freeland, and L. C. Kimerling, Phys. Rev. Lett. **54**, 2639 (1985).
[38] M. Stavola, in *Early Stages of Oxygen Precipitation in Silicon*, edited by R. Jones (Kluwer Academic, The Netherlands, 1996), p. 223.
[39] See Ref. 36 for detailed discussion of allowed $1s \rightarrow 2p_{0,\pm}$ transitions under $\langle 110 \rangle$ stress.